# $KNbO_3$ Single Crystals and Thin Films for SAW and BAW Devices

Kiyoshi Nakamura and Shigeo Ito
Graduate School of Engineering, Tohoku University, Sendai 980-8579, Japan

*Abstract* - In demand for low-loss wide-band communication devices, Potassium niobate ($KNbO_3$) is now receiving renewed interests because it has been found to exhibit high electromechanical coupling. This paper describes the optimum cuts of $KNbO_3$ for bulk acoustic waves (BAW) and surface acoustic waves (SAW) devices, with expectation of their application in the future. In addition, our recent works on growth of $KNbO_3$ thin films deposited by electron-cyclotron-resonance-assisted pulsed laser deposition (ECR-PLD) and the characterization are presented.

## I. INTRODUCTION

Piezoelectric crystals such as lithium niobate ($LiNbO_3$) and lithium tantalate ($LiTaO_3$) have been widely used in electronic and communication devices. In these applications piezoelectric materials are the most important and fundamental elements and their characteristics affect the device performance. One important parameter that determines the performance of piezoelectric devices is the electromechanical coupling factor of piezoelectrics. To achieve a higher sensitivity and a broader bandwidth, the advent of new piezoelectric materials with a higher electromechanical coupling factor has long been desired.

$KNbO_3$ crystal, known as an excellent nonlinear optic and electro-optic material, is now receiving renewed interests because it has recently been reported that $KNbO_3$ single crystal has by far higher coupling factors for surface acoustic waves [1, 2] and bulk acoustic waves [3, 4] as compared to those of $LiNbO_3$ or $LiTaO_3$. Moreover, $KNbO_3$ does not include toxic Pb. This is an attractive feature of $KNbO_3$, as Pb-free piezoelectrics will become increasingly more important.

This paper describes the optimum cuts for BAW and SAW devices of $KNbO_3$ single crystals, and growth of $KNbO_3$ thin films by ECR-PLD.

## II. $KNbO_3$ SINGLE CRYSTALS

Since the discovery of ferroelectricity in $KNbO_3$ crystal [5] by Matthias in 1949, a lot of works have been published on the crystal structure [6-8], crystal growth [9-11] and domain structures [12-14]. Piezoelectricity of $KNbO_3$ was measured by Wiesendanger [15] in 1974 and a high shear-mode coupling factor of 88% was reported. Since almost all fundamental physical constants of $KNbO_3$ were recently determined by Zgonic et al. [16], it became possible to calculate the piezoelectric properties using them.

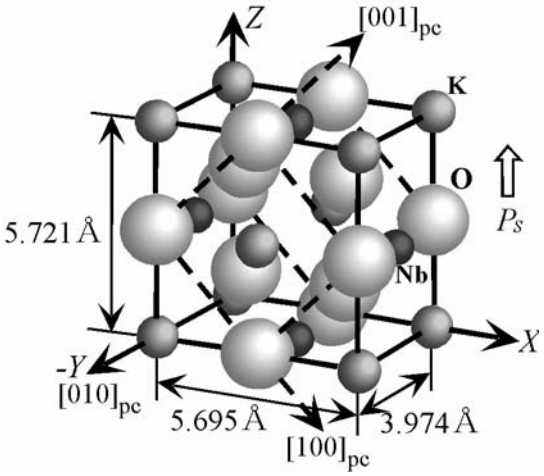


Fig. 1. Unit cell of orthorhombic $KNbO_3$ crystal.

$KNbO_3$ belongs to the point group mm2 of the orthorhombic system at room temperature and undergoes a sequence of phase transitions from the cubic phase to tetragonal, orthorhombic, and rhombohedral phases with decreasing temperature, i.e. at 435°C, 225°C, and -10°C [8], respectively. The orthorhombic single-crystal of $KNbO_3$ has a pseudocubic perovskite structure,

whose unit cell is schematically shown in Fig. 1, along with the crystallographic coordinate system (*X, Y, Z*) and the pseudocubic axes indicated by the subscript "pc". The pseudo-cube is being slightly elongated along the Z-axis parallel to the spontaneous polarization Ps.

$KNbO_3$ single crystals are usually grown from a $K_2CO_3$-$Nb_2O_5$ melt with excess $K_2CO_3$ acting as a flux by the Kyropoulos technique or the TSSG (top-seeded solution growth) technique. At present $KNbO_3$ crystals with dimensions of about 50×50×25 $mm^3$ are commercially available from some manufacturers.

*Optimum cuts for BAW devices*

We have theoretically calculated the orientation dependence of electro-mechanical coupling factors of $KNbO_3$ crystals for various modes of vibrations [3]. $KNbO_3$ single crystals exhibit very high coupling for most of these modes. Figure 2 shows the orientation dependence of the effective coupling factors for the thickness modes, $k_t$ and $k_s$, in the $\theta$ rotated *X*-cut about the *Y*-axis. The coupling factor for the thickness-extensional mode, $k_t$, is as high as 69% at the 49.5° rotated *X*-cut [3]. This value of $k_t$ is the highest among all known piezoelectrics, including PZT ceramics and even PZN-PT crystals which are now receiving attention because of their large coupling [17, 18]. To confirm the high coupling factor, an experiment was performed on the thickness-extensional mode of the 49.5º rotated *X*-cut plate. Figure 3 shows the frequency response of electrical impedance for a 49.5º rotated *X*-cut $KNbO_3$ crystal of 9.6×13.2×0.51 $mm^3$. The measured coupling factor is as high as 70%. At $\theta$ = 51.6°, the coupling factor for the thickness-shear mode, $k_s$, is zero, while $k_t$ is almost the same as the maximum value. Thus, this cut is useful for excitation of longitudinal waves, because no shear wave is generated. Rotated *X*-cut $KNbO_3$ plates around $\theta$ =50° would be promising as piezoelectric vibrators for various applications, such as high frequency ultrasonic transducers [19, 20].

The thickness-shear mode coupling factor, $k_s$, is maximum for the *X*-cut, which is 88.3%. This extremely large value agrees well with that measured by Wiesendanger [15]. The *X*-cut is useful for shear wave transducers and resonators.

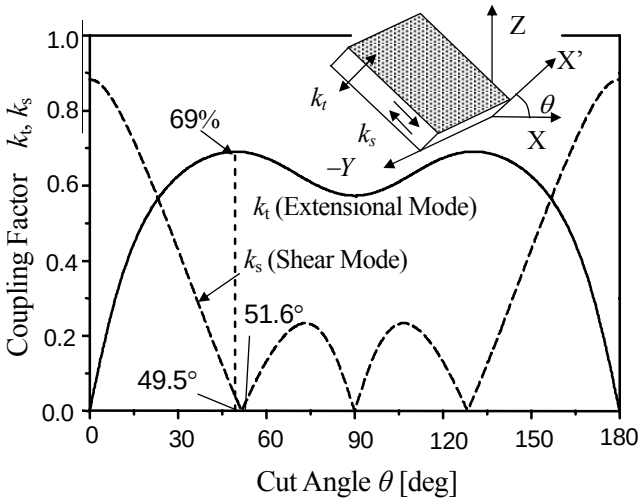


Fig. 2. Orientation dependence of coupling factors, $k_t$ and $k_s$, in a rotated *X*-cut $KNbO_3$ plate.

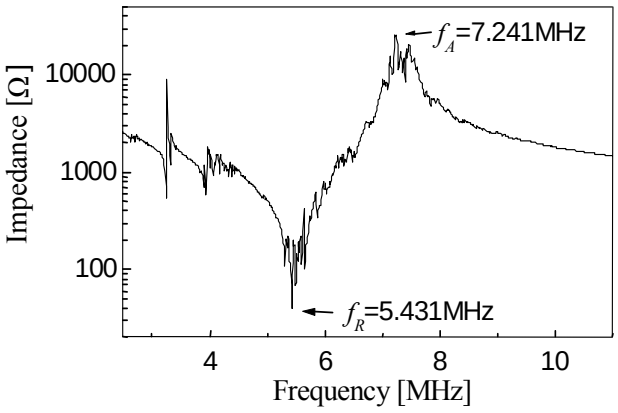


Fig. 3. Electrical impedance response for the thickness-extensional mode of a 49.5º-rotated *X*-cut plate.

The coupling factors for some other vibration modes are shown in Fig. 4. The piezoelectric transverse-effect coupling factor is as high as 58.8%, while the measured value is about 57%. The piezoelectric longitudinal effect coupling factor for the width-extensional mode in a thin plate with a finite width is 82.4%, which is close to that of PZN-PT (84%) [21]. The width-extensional mode vibrator is useful for array-type ultrasonic transducers.

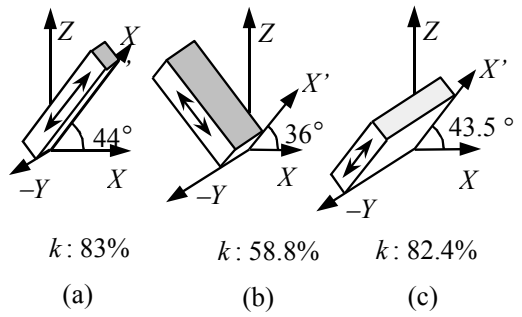


Fig. 4. Some important cuts and their coupling factors.

*Optimum cuts for SAW devices*

Yamanouchi et al. [1] have reported that the electromechanical coupling factor $k^2$ of the Rayleigh-mode surface wave on the *Y-X* $KNbO_3$ substrate is very high, about 0.53. The large coupling factor is very attractive for practical SAW devices, because it makes possible to obtain broadband low-loss SAW devices that cannot be realized with other piezoelectric substrates. They also reported that for 45º-75° rotated *Y*-cut a vanishing temperature coefficient of delay could be attained at room temperature [22] and that a SAW convolver using a 60° *Y*-cut exhibited an efficiency about 20dB higher than that of *Y-Z* $LiNbO_3$ [23].

We have shown that the BGS surface wave similar to that in 6mm crystals can exist on a rotated *Y*-cut about the *Z*-axis, which is called the "*Z*-axis cylinder" [2]. The calculated phase velocity for the metalized surface, $V_m$, and that for the free surface, $V_f$, are shown in Fig. 5 as functions of cut angle $\theta$, where $V_R$ is the velocity of the piezoelectrically inactive Rayleigh wave and $V_s$ is the bulk shear wave velocity. The SH-mode surface wave for the metalized surface exists in all orientations. In contrast, that for the free surface exists only in the very vicinities of $\theta$=0° and $\theta$=90°. The velocity $V_f$ shown in Fig. 5 represents the velocity minimizing the absolute value of the boundary condition determinant. One feature seen from Fig. 5 is that the BGS wave for the metalized surface has a velocity lower than the Rayleigh wave for $\theta$<62° and also lower than the *X'*-propagating bulk wave for any $\theta$. This suggests that the BGS wave is not leaky for off-axis propagation on the *Z*-axis cylinder substrate. Another feature is that the velocity for the free surface, $V_f$, at $\theta$=0° is about 1000 m/s lower than the bulk shear wave velocity $V_S$. This situation is quite different from the case of the BGS wave in 6mm crystals, which has a free-surface velocity very close to the bulk shear wave velocity $V_S$. The effective electromechanical coupling factor $k^2$ was calculated using following equation although it is not clear whether this expression is exactly applicable to the BGS wave in $KNbO_3$.

$$k^2 = \frac{2(V_f - V_m)}{V_f} \tag{1}$$

The coupling factor $k^2$ varies dramatically from a very large value of 0.53 for *Y-X* $KNbO_3$ to a relatively small value of 0.026 for *X-Y* $KNbO_3$.

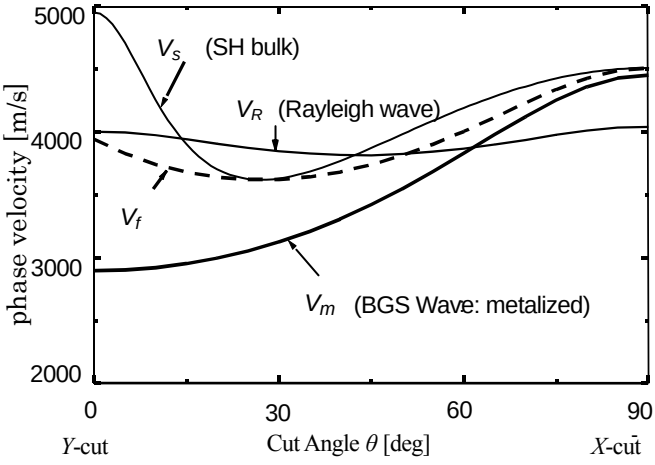


Fig. 5. BGS wave velocities in *Z*-axis cylinder cuts of $KNbO_3$.

## II. $KNbO_3$ THIN FILMS

Since the growth of $KNbO_3$ thin films for optical application was reported at the beginning of 1990, the films have been mainly fabricated on MgO or $SrTiO_3$ substrates using various techniques such as sputtering [24, 25], sol-gel [26], pulsed laser deposition (PLD) [27, 28], MOCVD [29, 30] or liquid phase epitaxy (LPE) [31, 32].

Table I. Deposition conditions for the films

| Parameter | Value |
|---|---|
| [K]/[Nb] ratio of the target | 2.0 |
| Oxygen pressure (Torr) | $6.0 \times 10^{-4}$ |
| Laser fluence (J/cm$^2$) | 3.5 |
| Laser repetition rate (Hz) | 10 |
| Substrate temperature ( ºC) | 700 |
| Target-substrate distance (mm) | 40 |
| ECR power (W) | 150 |

Recently, we have performed growth of $KNbO_3$ thin films on (100) MgO and (100) La-doped $SrTiO_3$ substrates using an electron-cyclotron-resonance-assisted pulsed laser deposition (ECR-PLD) technique [33]. The 266-nm-wavelength fourth harmonic from a pulsed Nd:YAG laser (Spectra Physics PRO 230, pulse duration =5 ns) was used to ablate the target materials. The deposited films tend to be K-deficient. This may be due to both scattering of potassium in the plume and re-evaporation after arriving at the substrate surface. To attain the stoichiometric [K]/[Nb] ratio in the deposited film, K-rich ceramic targets were used. The main parameters are listed in Table I. Figure 6(a) shows the X-ray diffraction (XRD) $\theta$-$2\theta$ pattern of the film deposited by ECR-PLD. It shows that the film is an orthorhombic (110)-oriented $KNbO_3$ film. The (110) lattice plane spacing of the film was calculated from the XRD data to be approximately 4.03 Å, which is very close to that of (110) $KNbO_3$ single crystal. Figure 7 shows the XRD rocking curve of the $KNbO_3$ (110) reflection. Its full width at half maximum (FWHM) is 0.83°, which indicates that the film quality is fine. The [K]/[Nb] ratio of the film was evaluated to be 0.97 using energy dispersive X-ray spectroscopy (EDS). To ascertain the effect of ECR on the growth of $KNbO_3$ films, a film was grown in an oxygen atmosphere without ECR activation (other conditions were the same as those shown in Fig. 6(a)). In Fig. 6(b) no peaks associated with $KNbO_3$ appeared. The peak at $2\theta \approx 47°$ was unable to be identified but may probably attributable to a $K_4Nb_6O_{17}$ phase, which has a lower [K]/[Nb] ratio. These results show that the ECR activation of oxygen is notably effective for epitaxial film growth and the ECR-PLD technique is capable of growing single-phase $KNbO_3$ films. The (110) $KNbO_3$ films are potentially suitable for high-frequency transducer, because the films correspond to the 45º-rotated *X*-cut about the *Y*-axis, which is close to the above-mentioned 49.5º-rotated *X*-cut and has a $k_t$ as high as 68% [3]. However, a bottom electrode is needed between the substrate-film interface to obtain such a transducer.

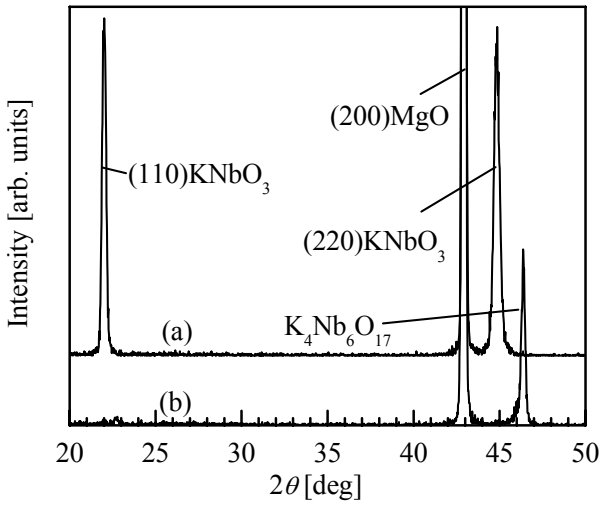


Fig. 6. XRD $\theta$-$2\theta$ patterns of (a) 0.69 μm-thick film deposited on (100) MgO by ECR-PLD and (b) 0.65 μm-thick film deposited on (100) MgO by PLD in an oxygen atmosphere without ECR activation.

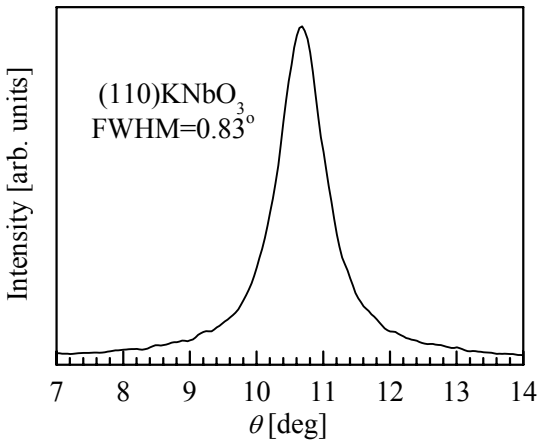


Fig. 7. XRD rocking curve of the (110) $KNbO_3$ film on (100) MgO. The film thickness was 0.69 μm

Alternatively we tried to generate a longitudinal bulk acoustic wave using an interdigital transducer (IDT) deposited on the (110) $KNbO_3$ film surface and poled by application of a dc voltage to it. The periodic length was 2.0 μm and the number of finger pairs was 30. The film polarizations in adjacent electrode-gap regions, as well as the RF electric fields, are opposite in sign to each other. Consequently the dilatational strains generated in all electrode-gap regions are in phase and contribute constructively to radiation of the longitudinal wave in the direction normal to the substrate. The transduction principle is similar to the "planar transducer" [34, 35]. Although the stoichiometric [K]/[Nb] ratio was achieved, the resistivity of the film was not sufficiently high for poling. To reduce the oxygen vacancies, the film was annealed for 3 h at 650ºC in a flowing $O_2$ atmosphere. As the result, the resistivity of the annealed film increased by a factor of $10^4$. The admittance response of the transducer was measured under the application of a 100 kV/cm dc bias, because the response became very small when the dc bias was removed. Figure 8 shows the electrical admittance response of the transducer. Small periodic peaks appeared at interval of about 9.5 MHz are the overtone thickness-extensional modes of the MgO substrate with a thickness of 0.5 mm. The velocity of the longitudinal wave was evaluated to be about 9500 m/s from the overtone frequencies. This velocity is close to the value calculated from the elastic constants of MgO [36]. In Fig 8 the overall admittance variation from 1.0 GHz to 1.5 GHz may be due to the radiation admittance of the Rayleigh wave [2]. The Rayleigh-wave velocity of (100) MgO substrate with a stress-free surface was estimated from its elastic constants to be approximately 5900 m/s. However, the measured velocity of the Rayleigh wave was about 4700 m/s. The velocity lowering may be attributable to the fact that the surface of the (100) MgO is covered with the (110) $KNbO_3$ film, whose velocity is lower than that of MgO. The effective coupling factor *k* calculated from the measured radiation conductance was about 9.8% for the film thickness of 0.69 μm (0.17λ, λ: SAW wavelength). If a higher quality thick film can be deposited, a higher coupling factor will be expected.

The (010) $KNbO_3$ films correspond to the *Z*-cut have been grown on (110) $SrTiO_3$ by Onoe et al. [30] and the SAW properties of the film have been reported by Yamanouchi et al [37]. However $KNbO_3$ films correspond to the "Z-axis cylinder cut" have not been grown yet. If a technique to control the orientation of films is established, $KNbO_3$ films would be practically useful for high-frequency SAW devices as an alternative to bulk crystals.

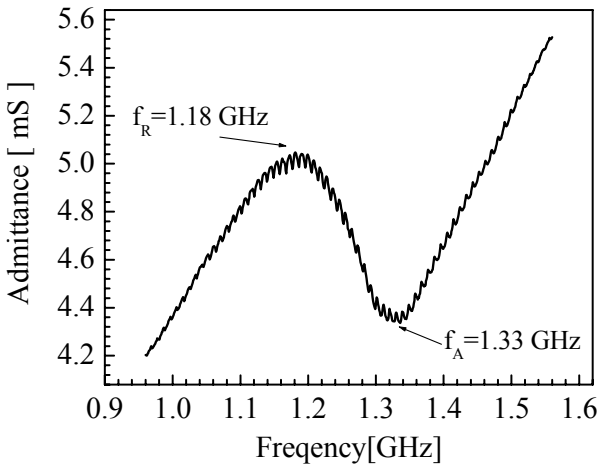


Fig. 8. Electrical admittance response of the (110) $KNbO_3$ film on (100) MgO measured under the application of a 100 kV/cm dc bias to the IDT.

## IV. CONCLUSIONS

The $KNbO_3$ crystal exhibits very high piezoelectric coupling for various vibration modes and surface acoustic waves, and therefore it would be attractive for piezoelectric applications. Its relatively low dielectric constants would make it easy to achieve impedance matching to generator and load impedances at high frequencies. Most of high-coupling materials include Pb as a component. $KNbO_3$ single crystals and thin films are lead-free and would therefore be expected to be promising for BAW and SAW devices in the future.

## V. REFERENCES

[1] K. Yamanouchi, H. Odagawa, T. Kojima and T. Matsumura: Electron. Lett. **33**, p.193 (1997).
[2] K. Nakamura and M. Oshiki: Appl. Phys. Lett. **71**, p.3203 (1997).
[3] K. Nakamura and Y. Kawamura: IEEE Trans.

Ultrason. Ferroelect. Freq. Contr. **47**, p.750 (2000).
[4] K. Nakamura and Y. Kawamura: Proc.1999 IEEE Ultrasonics Symposium, p.1013 (1999).
[5] B. T. Matthias: Phys. Rev. **75**, p.1771 (1949).
[6] B. T. Matthias and J.P.Remeika: Phys. Rev. **82**, p.727 (1951).
[7] E. A. Wood: Acta Cryst. **4**, p.353 (1951).
[8] G. Shirane, H. Danner, A. Pavlovic and R. Pepinsky: Phys. Rev. **93**, p.672 (1954).
[9] A.Reisman and F.Holtzberg: J. Amer. Chem. Soc. **77**, p.2115 (1955).
[10] C.E. Miller: J. Appl. Phys. **29**, p.233 (1958).
[11] J.J.Hurst and A.Linz: Mat. Res. Bull. **6**, p.163 (1971).
[12] K. G. Deshmukh and S. G. Ingle: J. Phys. D: Appl. Phys. **4**, p.124 (1971).
[13] K. G. Deshmukh and S. G. Ingle: J. Phys. D: Appl. Phys. **4**, p.1633 (1971).
[14] E. Wiesendanger: Czech. J. Phys. B **23**, p.91 (1973).
[15] E. Wiesendanger: Ferroelectrics **6**, p.263 (1974).
[16] M. Zgonik, R. Schlesser, I. Biaggio, E. Voit, J. Tscherry and P. Günter: J. Appl. Phys. **74**, p.1287 (1993).
[17] J. Kuwata, K. Uchino and S. Nomura: Jpn. J. Appl. Phys. **21**, p.1298 (1982).
[18] S. E. Park and T. R. Shrout: J. Appl. Phys. **82**, p.1804 (1997).
[19] N.M. Kari, T.A. Ritter, S.E. Park, T.R. Shrout and K.K. Shung: Proc. 2000 IEEE Ultrason. Symp. p.1065 (2000).
[20] K. Nakamura, T. Tokiwa and Y. Kawamura: Proc. Int. Conf. on New Piezoelectric Materials and High Performance Acoustic Wave Devices. p.13 (2002).
[21] S. Saitoh, T. Kobayashi, K. Harada, S. Shimanuki and Y. Yamashita: Jpn. J. Appl. Phys., **37**, p.3053 (1998)
[22] H. Odagawa and K. Yamanouchi: Jpn.J.Appl.Phys. **37**, p.2929 (1998).
[23] K. Yamanouchi, H. Odagawa, K. Morozumi and Y.Cho: Jpn. J. Appl. Phys. **37**, p.2933 (1998).
[24] T. M. Graettinger, S. H. Rou, M. S. Ameen, O. Auciello and A. I. Kingon: Appl. Phys. Lett. **58**, p.1964 (1991).
[25] S. Schwyn Thöny, H. W. Lehmann and P. Günter: Appl. Phys. Lett. **61**, p.373 (1992).
[26] G. J. Derderian, J.D. Barrie, K. A. Aitchison, P. M. Adams and M. L. Mecartney: J. Am. Ceram. Soc. **77**, p.820 (1994).
[27] C. Zaldo, D. S. Gill, R. W. Eason, J. Mendiola and P. J. Chandler: Appl. Phys. Lett. **65**, p.502 (1994).
[28] H. M. Christen, L. A. Boatner, J.D. Budai, M. F. Chisholm, L. A. Géa, P. J. Marrero and D. P. Norton: Appl. Phys. Lett. **68**, p.1488 (1996).
[29] M. J. Nystrom, B. W. Wessels, D. B. Studebaker, T. J. Marks, W. P. Lin and G. K. Wong: Appl. Phys. Lett. **67**, p.365 (1995).
[30] A. Onoe, A. Yoshida and K. Chikuma: Appl. Phys. Lett. **69**, p.167 (1996).
[31] R. Gutmann, J. Hulliger, Cryst. Prop. Prep. **32-34**, p.117 (1991).
[32] K. Kakimoto, S. Ito, I. Masuda and H. Ohsato: Jpn. J. Appl. Phys. **41**, 11, p.6908 (2002).
[33] T. Arai, S. Ito, K. Ishikawa and K. Nakamura: Jpn. J. Appl. Phys. **42**, p.6019 (2003).
[34] L. J. van der Pauw: Appl. Phys. Lett. **9**, p.129 (1966).
[35] K. Nakamura, H. Shimizu and N. Sato: IEEE. Trans. Sonics. Ultrasonics. **30**, p.345 (1983).
[36] S. S. Jaswal and V. D. Dilly: Solid State Communications. **24**, p.577 (1977).
[37] H. Odagawa, K. Kotani, Y. Cho and K. Yamanouchi: J. Appl. Phys. **38**, p.3725 (1999).